

HYDROTHERMAL CONVECTION AT SLOW-SPREADING MID-OCEAN RIDGES

UDO FEHN and LAWRENCE M. CATHLES *

*Department of Geological Sciences, Harvard University, Cambridge, Mass. 02138 (U.S.A.)
Ledgemont Laboratory, Kennecott Copper Corporation, Lexington, Mass. 02173 (U.S.A.)*

(Submitted January 19, 1978; accepted for publication July 24, 1978)

ABSTRACT

Fehn, U. and Cathles, L.M., 1979. Hydrothermal convection at the slow-spreading mid-ocean ridges. In: J. Francheteau (Editor), *Processes at Mid-Ocean Ridges*. Tectonophysics, 55: 239–260.

The discrepancy observed between measured heat flow data and the heat flow predicted by thermal models of mid-ocean ridges is commonly explained by the presence of hydrothermal convection in young oceanic crust. Numerical modelling of fluid flow through porous media has been used to investigate what permeability, depth of penetration and mass fluxes are necessary to produce conductive heat flow distributions compatible with observed heat flow data at spreading centers. The results presented here were calculated for oceanic crust between 0 and 2 m.y. old at a mid-ocean ridge with a half-spreading rate of 1 cm/yr.

The calculations show that theoretical and observed heat flow near mid-ocean ridges can be brought into better agreement if non-uniform rather than uniform permeability is assumed in the oceanic crust. If the crustal permeability is uniform, the percentage of heat flow values ($\geq 25\%$) which are increased by upwelling flow above the predicted values is significantly higher than that observed at mid-ocean ridges ($< 10\%$). If — due to faulting, for example — zones of high permeability exist in crust of low permeability, upwelling flow can be concentrated and the area of increased heat flow can be greatly reduced. In the latter case, the percentage of sea floor near mid-ocean ridges ($\geq 90\%$) where heat flow is depressed below the predicted values corresponds well with observed heat flow distributions near active spreading centers.

Average temperatures in crust with hydrothermal convection are considerably lower than those in purely conductive crust. This difference in average temperatures should result in crestal offsets at mid-ocean ridges. The observation that crestal offsets attributable to convective cooling are not larger than 50 m suggests that the depth of penetration of convection strong enough to produce conductive heat flow compatible with observed heat flow distributions is less than 5 km in crust younger than 2 m.y.

The downward flow of cold ocean water into the sea floor greatly reduces conductive heat flow. The magnitude of this inflow and hence the degree of heat flow reduction depends on the average permeability of the oceanic crust. Comparison of heat flow measurements from the FAMOUS area and from the Galapagos Spreading Center to heat flow over downwelling areas in our models indicates that the average permeability

* Present address: Department of Geosciences, Pennsylvania State University, University Park, Pa. 16802 (U.S.A.)

(including faults or high permeability zones) in young oceanic crust is not larger than 2.5 millidarcy.

Finally, the integrated mass flux through sea floor between 0 and 2 m.y. old was found to be approximately $4 \cdot 10^6$ g yr⁻¹ (cm of ridge). If this mass flux is considered representative for spreading centers and if older crust is included into the calculations, a total mass of $\sim 1 \cdot 10^{17}$ g yr⁻¹ is convected through the worldwide system of mid-ocean ridges.

INTRODUCTION

Much evidence suggests that hydrothermal activity is associated with the emplacement of new oceanic crust along mid-ocean ridges. Numerous pieces of hydrothermally altered basaltic and ultramafic rocks have been dredged from ridge areas, and the metalliferous sediments from these regions, particularly those in the vicinity of the East Pacific Rise, are best explained as the products of hydrothermal activity. Strong support for this hypothesis comes also from the recent discovery of active hydrothermal vents at the axis of the Galapagos Spreading Center (Von Herzen et al., 1977).

The presence of hydrothermal activity at spreading centers implies that convective as well as conductive heat transfer contribute to the cooling of newly formed oceanic crust. Consequently, the discrepancy observed between measured conductive heat flow and heat flow predicted by thermal models of mid-ocean ridges (e.g., Lister, 1972 and Morgan, 1975) as well as the great variability of closely-spaced heat flow measurements in these areas (Williams et al., 1974; Williams et al., 1977; Davis and Lister, 1977) are commonly attributed to hydrothermal convection in young oceanic crust. Estimates of the total difference between measured and predicted heat transfer at mid-ocean ridges range from $24 \cdot 10^{18}$ cal/yr to $65 \cdot 10^{18}$ cal/yr (Anderson et al., 1977; Wolery and Sleep, 1976; Williams and Von Herzen, 1974). The age of the ocean floor where measured and predicted heat flow begin to coincide varies between 5 m.y. for the Galapagos Spreading Center and 70 m.y. for the Atlantic Ocean (Anderson et al., 1977). This observation suggests that hydrothermal convection can occur in old crust far beyond the direct influence of hot intrusions at the axis of spreading centers.

While the presence of hydrothermal convection at mid-ocean ridges is commonly accepted, the precise manner in which this convection resolves the discrepancy between theoretical and observed heat flow is not well understood. In particular, since hydrothermal convection causes not only reduction of heat flow by the inflow of cold ocean water but also increase of heat flow by the exit of heated water, convection implies the existence of zones where heat flow is raised above the predicted values. The observation, that only a small percentage (<10%) of the heat flow values measured at mid-ocean ridges is higher than predicted, is an important constraint for models of hydrothermal convection at mid-ocean ridges.

A major obstacle to a better understanding of convection at mid-ocean ridges is the lack of knowledge about permeability and permeability distribution in oceanic crust. Estimates of the average permeability of oceanic

crust range from 0.45 mD (1 millidarcy = 10^{-11} cm²) (Ribando et al., 1976) to 10 mD (Anderson et al., 1977). The permeability in highly fractured parts of the oceanic crust was suggested to be as high as 10 darcy (Lister, 1974). Sediments are probably less permeable than fractured basement rocks; a range of 0.1 to 0.001 mD is given by Bryant et al. (1974), and a permeability of 0.25 mD was measured for a sediment sample from the Juan de Fuca Ridge (Pearson and Lister, 1973).

Qualitative explanations for patterns of hydrothermal convection associated with mid-ocean ridges have assumed either a uniform permeability of the oceanic crust (e.g., Lister, 1972) or flow through isolated fractures (Bodvarsson and Lowell, 1972). Similarly, two distinct types of quantitative models have been developed: Ribando et al. (1976) simulated the periodic heat flow distribution found by Williams et al. (1974) near the axis of the Galapagos Spreading Center by use of a continuum Darcy flow model with homogeneous permeability. Lowell (1975) investigated the effect of an isolated fracture loop on the heat flow distribution near a ridge system. Both of these models assumed a constant heat supply from below, and did not take into account the horizontal heat flow from narrow dike intrusions at the axis of spreading centers. The cooling of a single narrow dike intrusion by seawater convection was studied recently by Lowell and co-workers (Lowell et al., 1977, Lowell and Patterson, 1979).

We present here results of a Darcy flow model which can be used to compute fluid convection through oceanic crust of homogeneous permeability as well as through crust where flow is dominated by isolated fractures or shear zones. In this paper, we investigate hydrothermal convection in crust younger than 2 m.y. and without sediment cover at a ridge with half spreading rate of 1 cm/yr. The purpose of this investigation is to find permeability distributions and penetration depths for fluid flow which are compatible with heat flow distributions and topography observed at mid-ocean ridges. The results are then used to estimate mass fluxes and temperature distributions associated with hydrothermal convection at active spreading centers.

THE NUMERICAL MODEL

The numerical model we used for the calculation of hydrothermal convection at mid-ocean ridges is essentially the same model developed previously by Cathles (1977) for hydrothermal systems associated with the cooling of hot plutons. The model is based on equations for balance of momentum (Darcy's Law):

$$-\nabla p + \rho \underline{g} - \frac{\nu}{k} \underline{q} = 0 \quad (1)$$

balance of mass:

$$\nabla \cdot \underline{q} = 0 \quad (2)$$

and balance of heat:

$$\rho_m c_m \frac{\partial T}{\partial t} = -\nabla \cdot q c_f T + K_m \nabla^2 T - \rho_m c_m \underline{v}_s \cdot \nabla T \quad (3)$$

where c_f = specific heat of fluid ($c_f = H/T$; H = enthalpy); c_m = specific heat of fluid saturated rock (0.2 cal/g dg); g = gravitational field strength (980 cm/sec²); k = permeability; K_m = thermal conductivity of fluid saturated rock ($6 \cdot 10^{-3}$ cal/dg cm sec); p = pressure; q = mass flux; v_s = half spreading rate (1 cm/yr); ν = kinematic viscosity; ρ_m = density of fluid saturated rock (2.7 g/cm³); ρ = density of fluid.

This system of equations is solved by standard finite difference techniques (Carnahan et al., 1969). An important feature of the model is that the pressure and temperature dependence of the kinematic viscosity, enthalpy and density of the circulating fluid (pure water) are taken into account (Cathles, 1977). The two-dimensional solution domains contain twenty grid points in the vertical z -direction and thirty points in the y -direction; the grid spacing of the model is variable and can be adjusted to the problem in question. All the calculations were carried out for a half-spreading rate of 1 cm/yr, an intrusion temperature of 1200°C, and a surface pressure of 200 bars corresponding to sea floor at 2000 m depth.

The above equations are applicable to cases of water convection through a homogeneous porous medium as well as through a system of interconnected fractures as long as the Reynolds numbers are smaller than 1 which was always the case in our calculations. In the case of flow through fractures, two approaches are possible: if flow takes place through fractures spaced less than a few hundred meters apart, the system can be modeled as flow through uniform porous media. When fracture spacings are in excess of a few hundred meters, the assumption that temperatures within matrix blocks between fractures are close to those calculated for a homogeneous porous medium is no longer valid. Convection can then be treated in terms of flow through individual zones of high permeability set in a matrix of low permeability.

BOUNDARY AND INITIAL CONDITIONS

The choice of boundary and initial conditions is of basic importance for the results of numerical models. The boundary conditions for fluid flow are obvious: no flow through the sides and through the base of the domain and free flow through the surface. The choice of temperature boundary conditions needs more discussion. Since our domain usually has a width of 20 km, horizontal heat flux through the right hand boundary due to a dike intrusion at the ridge axis (left hand boundary) is small and can be neglected. The right hand boundary of the domain was thus assumed to be insulating. The heat flow through the base of the domain was chosen to be constant at 6 HFU (1 HFU = 10^{-6} cal/cm² sec). This heat flow is increased by the heat

flow from the ridge axis to a total average heat flow of approximately 15 HFU through the surface of the domain (see for example Fig. 3). The surface of the domain was kept at a constant temperature of 0°C. This boundary condition formally requires all heat flow at the surface to be conductive, although in a real situation this total heat flow may be partly conductive and partly convective. As an approximation to this real situation, we compute total and conductive heat flow at the first grid point which is less than 100 m below the surface. Total heat flow at this depth is a good estimate of the total heat flow through the surface, while the conductive contribution gives a useful measure of the minimum conductive heat flow in upwelling areas and of the maximum conductive heat flow in downwelling areas.

At the ridge axis, a boundary condition suggested by Oldenburg (1975) was chosen in most of our calculations:

$$-K_m \frac{\partial T}{\partial y} = \rho_m v_s (L + (T_m - T_f(t, z))c_m) \quad (4)$$

where L = latent heat (100 cal/g); T_m = intrusion temperature (1200°C); T_f = temperature at the left hand (ridge) boundary. The temperature T_f at a particular timestep t_n was chosen to be the temperature at the ridge boundary calculated for the previous timestep t_{n-1} . This boundary condition assumes a continuous spreading process at the ridge axis. Another possibility for simulating sea floor spreading at a rate of 1 cm/yr is the periodic intrusion of dikes of 200 m width at the ridge axis in time intervals of 20,000 years. Since evidence for such a periodicity has been found at the Mid-Atlantic Ridge (Moore et al., 1974, Ballard and Van Andel, 1977), this model was also tested.

To test the boundary conditions chosen and to evaluate the time necessary to reach steady state conditions, the evolution of fluid convection with time is compared for the following four cases, all computed for domains of 20 km width and 10 km depth and with a constant heat flow of 6 HFU from below:

(1) Intrusion of a dike of 200 m width and 9.5 km height at the ridge axis. The initial temperature in the domain of 0.25 mD uniform permeability was assumed to correspond to a heat flow of 6 HFU, i.e. 1000°C at the base, linearly decreasing to the surface. Intervals between intrusions were 20,000 years long.

(2) Heat flow from the ridge axis as given by equation (4) into a domain of 0.25 mD homogeneous permeability. Initial temperature of 1000°C at the base, linearly decreasing to the surface.

(3) Like case 2, but with initial temperature of 500°C at the base, linearly decreasing to the surface.

(4) Like case 2, but with uniform permeability of 0.5 mD in the domain.

The development with time of the average temperatures in the domain is demonstrated for these four cases in Fig. 1. Case 1, periodic intrusion at the ridge axis, begins at an average temperature of 500°C which is increased to

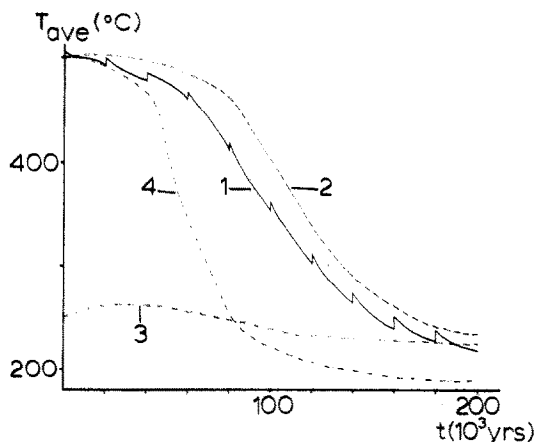


Fig. 1. Evolution of average temperatures with time in domains of 10 km depth and 20 km width. See text for description of cases 1–4.

507°C due to the intrusion of a 200 m wide dike at 1200°C. Convection causes a decrease in average temperature to 493°C before the next episode of intrusion which increases the average temperature to 499°C, and so on. After about 50,000 years, the average temperature of the crust in the domain begins to decrease rapidly until a quasi-steady state temperature of about 225°C is reached.

The evolution with time of the average temperature in case 2, continuous intrusion at the ridge axis, follows the trend of case 1 except for the somewhat later beginning of the decrease in average temperature. In case 3, where an initial average temperature of 250°C was chosen, variation of the average temperature with time is small. These three cases, all of which have domains with uniform permeabilities of 0.25 mD, reach steady state average temperatures around 230°C. If a higher uniform permeability of 0.5 mD is assumed (case 4) a sooner and steeper decline in average temperature results, and the steady state average temperature is reduced to 190°C.

The variation with time of total fluid mass efflux through the surface of the domain is compared in Fig. 2a for the four cases. The mass efflux is integrated over the width of the domain and given in 10^6 g/yr (cm of ridge axis). In a similar diagram (Fig. 2b), heat flow through the surface is plotted, also integrated over the width of the domain and given in cal/cm sec. Most of the mass flux shortly after the onset of convection is associated with the steep horizontal temperature gradients close to the ridge axis. After some time, several other convection cells develop in the domain which give rise to additional discharge areas. The increase of heat flow and mass flux caused by these additional convection cells coincides with the steep decline in average temperatures shown in Fig. 1. This decrease in average temperatures and the corresponding transient increase in mass flux and heat flow represents the fact that — because convective heat transfer is more efficient than conduc-

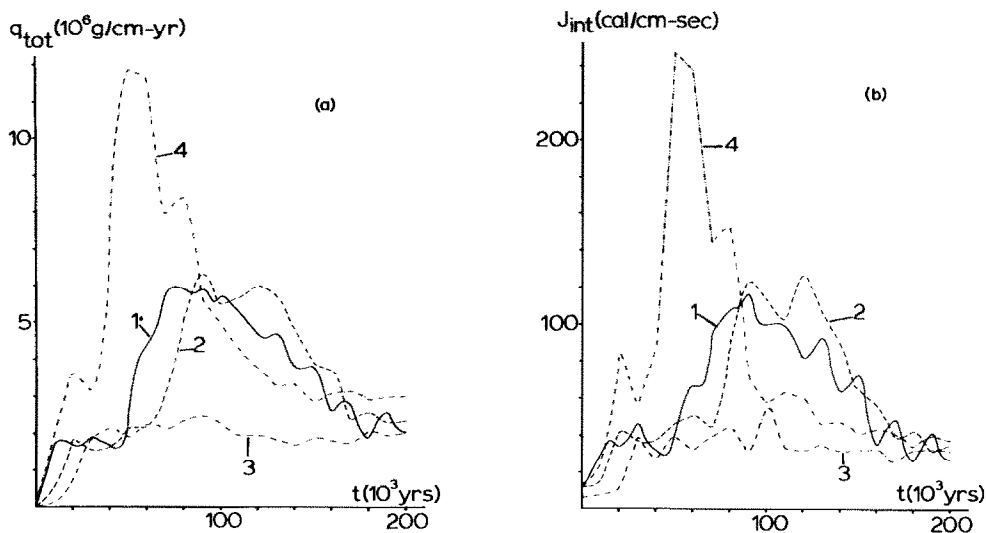


Fig. 2. Time evolution of integrated mass fluxes (a) and of integrated heat fluxes (b) through surface of 10 km deep and 20 km wide domain. See text for description of cases 1–4.

tive one — the heat stored and, correspondingly, the average temperature of the crust are higher in a purely conductive layer than in the same layer, if fluid convection takes place.

The comparison of these four cases suggests the following conclusions in regard to the choice of boundary and initial conditions for our models. First, the similarity of average temperatures, mass fluxes and heat fluxes found for the cases 1 and 2 indicates that the heat flow boundary condition (4) is a proper way to represent the intrusion of new oceanic crust at mid-ocean ridges. Since the boundary condition (4) is more flexible in choice of time steps and grid spacing than a periodic intrusion at the ridge axis, this boundary condition was chosen for the further calculations. Secondly, the observation that cases 1, 2 and 3 achieved very similar steady state temperatures, mass fluxes, and heat fluxes indicates that the solutions converge and reach steady state within $\sim 200,000$ yrs. This time span required to obtain steady state is short compared to the lifetime of spreading centers which usually have been spreading for millions of years. Steady state solutions should thus be typical for slow-spreading ocean ridges active today. Steady state in this context means that convection cells are fixed with respect to the ridge axis. This assumption implies that oceanic crust goes through zones of upwelling and downwelling convection and, correspondingly, through zones of high and low heat flow as it moves away from the ridge axis. Support for this assumption is offered by measurements made by Katz et al. (1977) who ascertained an oscillatory behavior of heat flow in drill core samples from the Mid-Atlantic Ridge.

FLUID CONVECTION FOR VARIOUS PERMEABILITY DISTRIBUTIONS IN THE OCEANIC CRUST

In Fig. 3, steady state temperature distribution, flow lines and heat flow are shown for crust with a uniform permeability of 0.25 mD (case 2). The ridge axis is at the left hand side of the domain of 10 km depth and 20 km width. Isotherms are shown in intervals of 100°C and stream lines in steps of 2.5 of the dimensionless stream function. A large convection cell driven by the horizontal temperature gradients at the ridge axis has developed. The convection cell has two discharge areas, one at the ridge axis with a width of

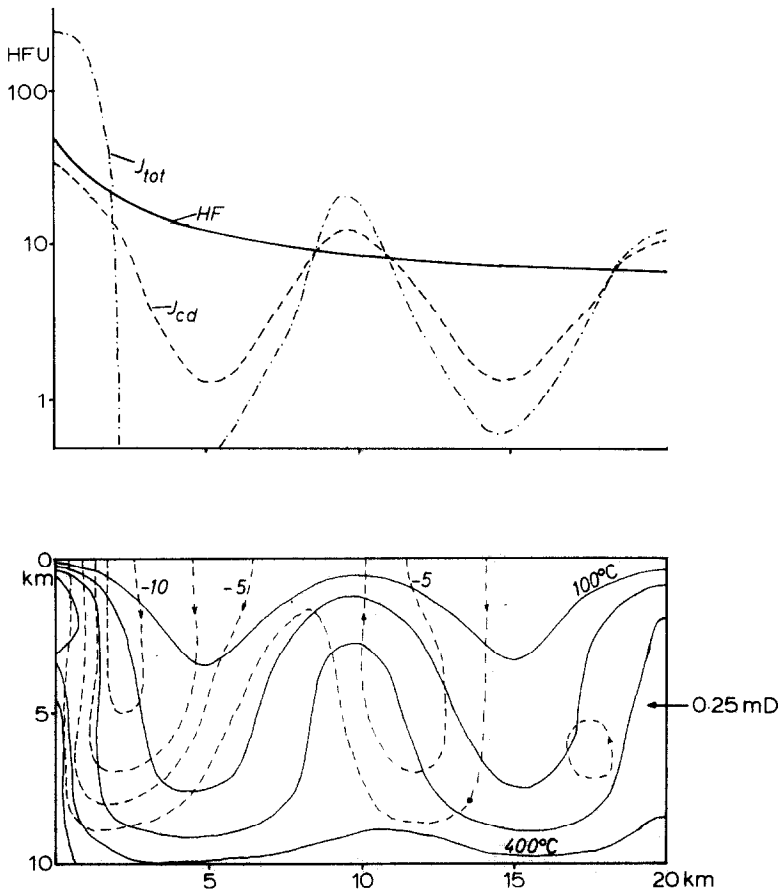


Fig. 3. Steady state temperatures and stream lines in crust of uniform 0.25 millidarcy permeability. Ridge axis is located at the left hand side of the domain. Total heat flow J_{tot} and conductive contribution J_{cd} , both calculated at a depth of 70 m, are compared to heat flow HF computed in absence of convection. Heat flow is given in heat flow units (1 HFU = 10^{-6} cal/cm² sec) on an exponential scale.

2.5 km and a second one at a distance of 10 km from the ridge axis. A weak counter cell has appeared at the right boundary of the domain. Temperatures in the domain are generally below 500°C, temperatures above 500°C are found only close to the ridge axis.

In the upper half of the diagram, heat flow through the surface is plotted against distance from the ridge axis. An exponential scale is used for the heat flow values which are given in HFU (1 HFU = 10^{-6} cal/cm² sec). Here and in the following diagrams, the total heat flow J_{tot} which is the sum of convective and conductive heat flow is plotted together with the conductive part J_{cd} , both calculated at a depth of 70 m. The conductive heat flow at the surface lies between these two curves. The exact breakdown between the conductive and convective portion of the total heat flow at the surface depends on fracture width and fracture spacing in a surface location. The curve *HF* indicates the heat flow distribution in absence of convection. In general, heat flow is depressed below the theoretical heat flow *HF* in areas of downwelling flow and is increased over discharge areas. Discharge areas cover approximately 30% of the surface of the domain in this case.

In Fig. 4, the flow pattern and isotherms are shown for a domain in which fluid flow is restricted to the upper five kilometers of the crust. The impermeable zone is separated by the heavy broken line from the permeable zone where a uniform permeability of 0.5 mD was assumed. Three separate convection cells can be distinguished, the main one convecting towards the ridge axis. The two weaker convection cells have discharge areas in distances of 10 and 20 km from the ridge axis. Temperatures in the impermeable part of the domain are very little affected by the convection and reach values of more than 1000°C at the ridge axis. In the permeable half of the domain, temperatures are below 500°C except for the area close to the ridge axis. The heat flow distribution is similar to the one of Fig. 3, but the discharge areas are somewhat narrower and cover only 25% of the surface area.

The assumption that oceanic crust is of uniform permeability is probably not a good representation of the situation at mid-ocean ridges. Since newly intruded magma is permeable to water circulation only after solidification and after contraction due to cooling has opened fractures, a temperature dependence of the permeability of oceanic crust is likely. The temperature at which cooling magma becomes permeable lies between 400°C and 800°C (Lister, 1974). Because temperatures in the convective part of the domain are generally lower than these cracking temperatures, it was found that models which took into account the impermeability of crust at temperatures above 500°C resulted in steady state distributions of temperatures and fluid flow very similar to those of models in which this temperature dependence of the permeability was neglected. This result assumes that the rate of propagation of a cracking front through newly intruded magma is faster than the average rate of intrusion, an assumption which is justified by calculations on the penetration of water into hot rock. Lister (1974, 1977) estimates that a cracking front propagates through cooling rock at rates between 2 and 60

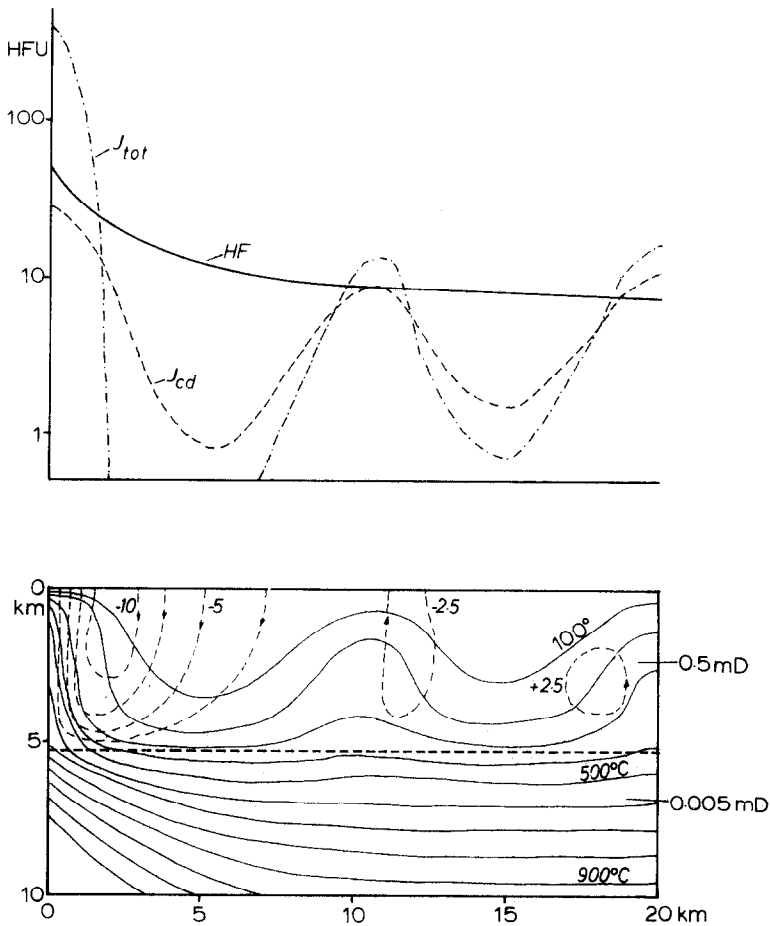


Fig. 4. Steady state temperatures, stream lines and heat flow distribution for domain of uniform permeability of 0.5 mD and penetration depth $h_p = 5$ km. Symbols in heat flow distribution as in Fig. 3.

m/yr. Thus, a dike of 200 m width which intrudes into an environment at temperatures steadily maintained by hydrothermal convection below the cracking temperature becomes permeable for fluid flow within a period of less than about 100 years. This time span is very short compared to the 10,000 to 20,000 years thought to elapse between episodes of intrusion at mid-ocean ridges (Moore et al., 1974).

The increase of pressure with depth probably also affects the openness of fractures to fluid flow. Since the existence of fractures depends not on the hydrostatic pressure but on the lithostatic pressure which can be approximated by a linear increase with depth, pressure dependence can be modeled as depth dependence. In Fig. 5, the flow pattern is shown resulting from a

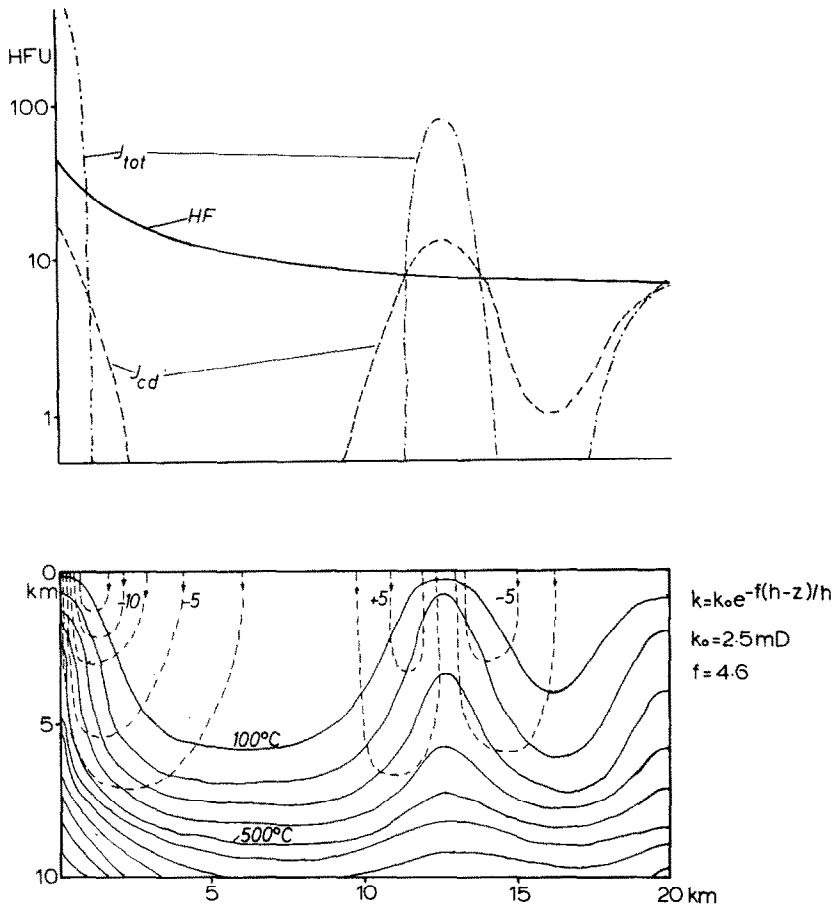


Fig. 5. Steady state temperatures, stream lines and heat flow distribution in crust where permeability decreases exponentially from surface permeability $k_0 = 2.5$ mD to base permeability $k_b = 0.025$ mD. Symbols in heat flow distribution as in Fig. 3.

permeability distribution which decreases exponentially with depth according to:

$$k(z) = k_0 \exp(-f(h - z)/h) \quad (5)$$

where k_0 = surface permeability; f = decay constant and h = depth of domain. The permeability in this case decreases from a surface permeability $k_0 = 2.5$ mD to a permeability of 0.025 mD at the base of the domain. A strong convection cell results at the ridge axis causing a large, narrow peak in the heat flow distribution. A second discharge area appears at a distance of 13 km from the ridge axis producing another sharp peak in the heat flow distribution. In the rest of the domain, isotherms are so much depressed that the heat flow over large parts of the domain is practically zero. As in the

previous cases, temperatures within the convection cells are smaller than 500°C , although flow is concentrated closer to the surface than in cases with homogeneous permeability distribution in the crust.

In all the cases so far, it was assumed that the crust has a uniform permeability in horizontal direction. The presence of numerous fissures at mid-ocean ridges (e.g., Ballard and Van Andel, 1977) and the observation of temperature anomalies above fissures (Crane and Normark, 1977) suggests, however, that fractures or shear zones are of fundamental importance for flow regimes in oceanic crust. The next three examples illustrate the effect fractures can have on the flow distribution. We modeled the flow through frac-

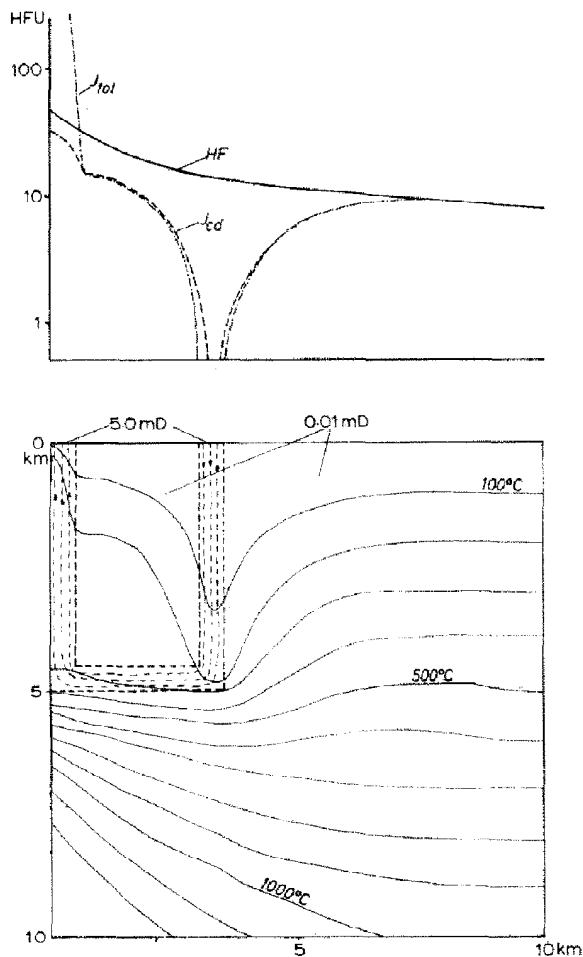


Fig. 6. Steady state temperatures, stream lines and heat flow distribution for loop of high permeability zones ($k = 5.0$ mD) in crust of low permeability ($k = 0.01$ mD). Symbols in heat flow distribution as in Fig. 3.

tures by introducing narrow zones of high permeability into a domain of low or intermediate permeability.

Figure 6 shows stream lines and isotherms for a fracture loop where 500 m wide zones of 5.0 mD permeability at the ridge axis and at a distance of 3 km from the ridge axis are connected by a similar zone of high permeability at a depth of 5 km. The rest of the domain has a permeability of 0.01 mD which practically prevents fluid flow. The fluid flow is thus restricted to the fracture loop; the flow direction is towards the ridge axis. Mainly the temperatures in the block between the fractures are affected by this kind of convection. Heat flow is depressed sharply over the downwelling branch of the fracture loop and reaches a high peak over the discharging branch. The influence of this kind of convection on the temperature distribution in the

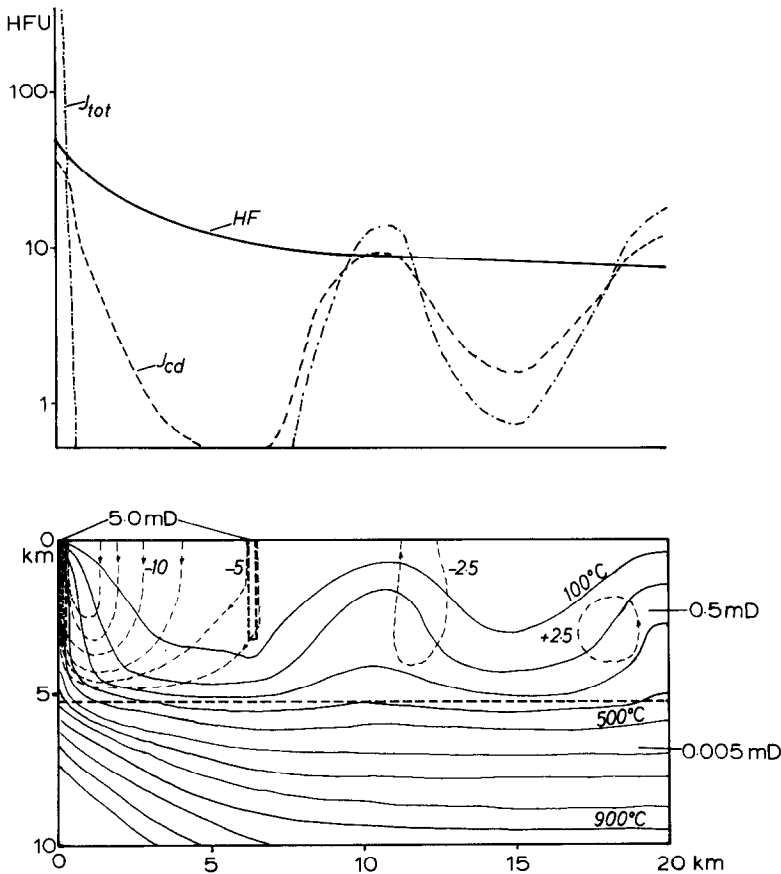


Fig. 7. Steady state temperatures, stream lines and heat flow distribution in crust of 0.5 mD permeability with 250 m wide zones of high permeability ($k = 5.0$ mD) at the ridge axis and in a distance of 6.25 km from the ridge axis. Symbols in heat flow distribution as in Fig. 3.

domain is negligible at distances greater than 5 km from the ridge axis.

A more realistic case is the situation where isolated zones of high permeability exist in a crust of otherwise low permeability. Fig. 7 and 8 illustrate the effect narrow zones of 5.0 mD permeability have on the flow distribution in the domain shown in Fig. 4, i.e., uniform permeability of 0.5 mD in the upper 5 km of the domain and very low permeability in the lower 5 km of the domain. In Fig. 7, two high permeability zones, each of which is 250 m wide and 3 km deep, are located at the ridge axis and at a distance of 6.5 km from the ridge axis, respectively, i.e., one zone is situated in the upwelling limb, the other in the downwelling part of the convection cell flowing towards the ridge axis. Almost the entire upwelling flow of this con-

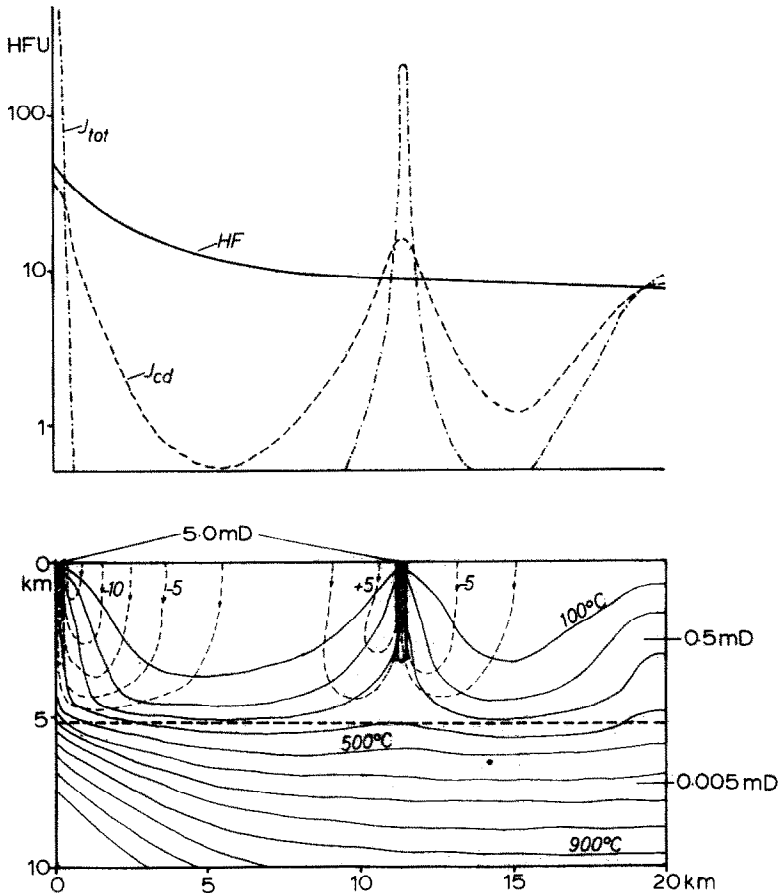


Fig. 8. Steady state temperatures, stream lines and heat flow distribution in crust of 0.5 mD permeability with 250 m wide zones of high permeability ($k = 5.0$ mD) at the ridge axis and in a distance of 11 km from the ridge axis. Symbols in heat flow distribution as in Fig. 3.

vection cell is concentrated in the zone of high permeability at the ridge axis. This concentration of fluid flow narrows the zone where heat flow is higher than HF to approximately 500 m as compared to 1.7 km in the case of uniform permeability (see Fig. 4). Although the high permeability zone in the downwelling part of the convection cell attracts some downwelling flow, it has only a small effect on fluid convection and heat flow distribution. Convection in the rest of the domain is not influenced by the presence of these two high permeability zones.

Fluid flow and heat flow distribution in the entire domain are strongly affected if the second zone of high permeability is located at a distance of 11 km from the ridge axis in the upwelling limbs of convection cells (Fig. 8). The two high permeability zones in this example attract practically the entire upwelling flow in the domain. Strong, narrow peaks in the heat flow distribution correspond to the discharge areas over the two high permeability zones. The percentage of the surface with heat flow higher than predicted is decreased to less than 10% of the domain as compared to 25% in the case of uniform permeability (see Fig. 4).

It is important to note that the concentration of upwelling flow into a fracture does not necessarily produce a similarly narrow zone of high heat flow. If the rock surrounding the fracture is impermeable an envelope of high conductive heat flow is caused by the high temperatures in the upwelling fluid (see Fig. 6). If, however, the surrounding rock is of a permeability which allows fluid flow, the steep horizontal temperature gradients around the fracture with upwelling flow induce downwelling flow very close to the fracture. This downwelling convection is what narrows the zone of high heat flow. The width of this zone depends on the width of the highly permeable zone and on the contrast in permeability between fracture and surrounding rock.

The presence of zones of high permeability in regions of upwelling flow influences not only the distribution of heat flow but also the mass flux through the surface. An increase of 23% in integrated mass flux was found for the model shown in Fig. 8 as compared to the mass flux through the surface of the same domain but without the high permeability zones (see Fig. 4). Interestingly, this increase in mass flux turns out to be proportional to the difference in average surface permeability between the two cases. Thus, it may be possible to estimate mass fluxes through a crust of non-uniform permeability by using the results obtained for domains with the same average, but uniform permeability.

The models shown in Figs. 6–8 are directly applicable only to cases where zones of high permeability are fixed with respect to the ridge axis. Examples for such cases are the area of the ridge axis itself and zones where plates go through episodes of high tectonic activity such as the uplift zones at the edges of a rift valley. In other cases, zones of high permeability may move with the moving plate. If the convection cells in permeable rock are indeed fixed with respect to the ridge axis, as suggested earlier, these fracture zones

would go through areas of upwelling and downwelling flow. Fig. 7 and 8 can then be interpreted as providing two views of convection in a plate with a high-permeability zone moving along with the plate.

DISCUSSION

In Fig. 9, the average temperatures in domains of 10 km depth and 20 km width are plotted against permeability. If only conductive cooling occurs in these domains, an average temperature, T_{cd} , of 720°C results. Convection in the domain lowers the average temperature considerably; the degree of this decrease in average temperature depends primarily on the penetration depth, h_p , of the convection and secondarily on the permeability in the crust. Average temperatures range between 580°C for cases with a penetration depth of 3 km and 190°C for cases with a penetration depth of 10 km. The two circles in the diagram show cases calculated for domains in which the permeability decreases exponentially over two orders of magnitude over the depth of the domain. These two cases and the case with two high permeability zones (see Fig. 8) indicated by the closed triangle are plotted at their respective average surface permeability.

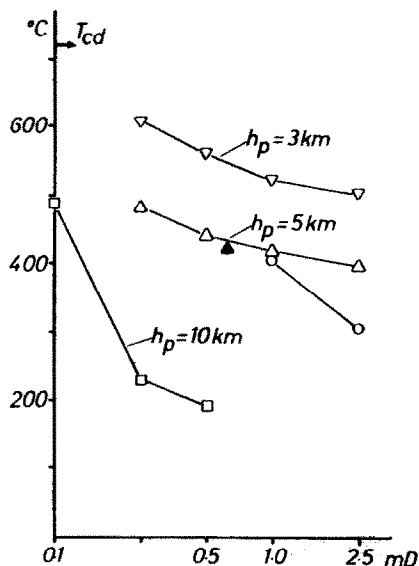


Fig. 9. Average steady state temperatures for oceanic crust between 0 and 20 km distance from the ridge axis and between 0 and 10 km depth below the sea floor for various permeabilities and fluid convection depths h_p . Open circles indicate cases where the permeability decreases exponentially with depth. The closed triangle shows the case (Fig. 8) where two zones of high permeability separated by 11 km exist in crust of 0.5 mD permeability. This case is plotted at its average surface permeability. The average temperature, T_{cd} , in absence of convection is indicated at the heat flow axis.

Convective cooling of the top 10 km of the oceanic crust has consequences for the relation between depth and age at mid-ocean ridges. The relation observed between depth and age of the sea floor can be explained by purely conductive cooling of oceanic crust as it moves away from a spreading center (e.g., Davis and Lister, 1974, and Parsons and Sclater, 1977). Since convective cooling of oceanic crust is not included in these models, the difference in average temperature between a purely conductive layer and layers with conductive and convective heat transfer (as illustrated in Fig. 9 for crust between 0 and 2 m.y. old) should result in a deviation from the depth-age relation close to spreading centers. The temperature difference between the conductive case and cases with convection can be converted into a crestal offset which — depending on the value of the thermal expansion coefficient of the crust — ranges between 26 m ($\alpha = 2.6 \cdot 10^{-5} \text{ dg}^{-1}$) and 40 m ($\alpha = 4 \cdot 10^{-5} \text{ dg}^{-1}$) per 100°C of temperature difference in the 10 km of the domain.

Hydrothermal convection not only causes a decrease in average temperatures near spreading centers but also alteration reactions in the crust some of which — as, for example, the serpentinization of peridotite — are accompanied by a considerable increase in volume (Coleman and Keith, 1971). The influence this volumetric increase may have on the elevation of mid-ocean ridges depends on the rate of hydrothermal alteration in the crust. If all the alteration occurs within the first 2 m.y., the volumetric increase due to alteration would probably result in an increase in height that would compensate the crestal offset due to contraction during convective cooling of the crust. In this case, only little deviation from the depth-age relation would be visible at mid-ocean ridge crests. If, however, hydrothermal alteration occurs over a longer period of time, expansion caused by this alteration produces a nearly constant offset of the elevation which does not affect the depth-age relationship. In the latter case, the temperature difference between conductive and convective regime would result in an observable crestal offset.

The crestal offset observed for the Mid-Atlantic Ridge is not larger than 250 m (Davis and Lister, 1974, Parsons and Sclater, 1977). Since about 200 m of this offset is attributable to horizontal heat conduction and changes in thermal parameters at the mantle-crust boundary (see discussion in Davis and Lister, 1974) contraction due to convective cooling in this example has to be less than about 50 m. We assume that hydrothermal alteration is not complete in 2 m.y. in this case because hydrothermal circulation is inferred to prevail in Atlantic crust up to 70 m.y. old (Anderson et al., 1977). Thus, because convection in regimes with penetration depths greater than 5 km result in contraction larger than 100 m, convection probably does not penetrate deeper than 5 km in crust younger than 2 m.y. in the Atlantic Ocean. Similar arguments can be used for other active spreading centers so that this limit of hydrothermal penetration is probably typical for most mid-ocean ridges.

Average temperatures show only a weak dependence on permeability and

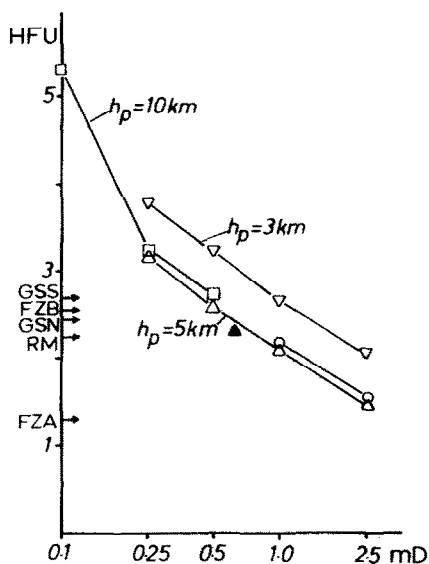


Fig. 10. Average steady state heat flow over areas with downwelling convection in crust of various permeabilities and penetration depths. Open circles and closed triangle as in Fig. 9. Average heat flow values in parts of the FAMOUS area and at the Galapagos Spreading Center are given as comparison; see text for explanation of symbols for these areas.

therefore do not usefully constrain the average permeability of oceanic crust. Heat flow distributions more directly reflect the permeability distribution of the crust. Because most of the heat flow values observed at mid-ocean ridges are lower than predicted by thermal models, they probably represent areas with downwelling convection and should be compared to heat flow values of areas with downwelling flow in our models. In Fig. 10, average values of conductive heat flow, J_{down} , over areas with downwelling convection in our models are plotted against permeability. The stronger convection associated with higher permeability in the crust causes a stronger decrease of temperatures in the downwelling parts of convection cells. Consequently, J_{down} decreases considerably with increasing permeability; the values of J_{down} range between 5.3 and 1.5 HFU.

In order to compare our results to observed heat flow values close to mid-ocean ridges, we used the heat flow distribution measured in the FAMOUS area of the Mid-Atlantic Ridge (Williams et al., 1977) and at the Galapagos Spreading Center (Williams et al., 1974, and K. Green, 1977, unpublished data). The results of the FAMOUS area are more applicable because the half-spreading rate of the Mid-Atlantic Ridge (0.9 cm/yr) is closer to that used in our calculations (1 cm/yr) than the half-spreading rate of the Galapagos Spreading Center (3.5 cm/yr). Heat flow values were measured in three separate parts of the FAMOUS area: fracture zone A (FZA), fracture zone B

(*FZB*) and in the western rift mountains (*RM*). The average heat flow values of these three areas and of the areas north (*GSN*) and south (*GSS*) of the Galapagos Spreading Center are indicated in Fig. 9. To insure that the average value calculated for these five areas represent heat flow over areas of downwelling convection, we included only heat flow values smaller than 5 HFU in the calculation of these averages. Since our models show that zones with weak downwelling convection can have heat flows significantly higher than 5 HFU, the restriction to values <5 HFU probably means that the averages calculated are minimum values for these areas.

Average heat flow J_{down} for fracture zone B, rift mountains and Galapagos Spreading Center fall into the range between 2.2 and 2.7 HFU while the value found for fracture zone A is considerably lower. Since 20 of the 35 stations in fracture zone A are given as "minimum value" only, the average value found for this area is probably underestimated. If the remaining four averages are considered as representative heat flow averages over downwelling areas close to mid-ocean ridges, they suggest that average permeabilities (including fractures) of young oceanic crust range between 0.25 and 2.5 mD.

Fig. 11. shows steady state mass fluxes through the surface of domains for crusts of various permeabilities. Mass fluxes are integrated over the first 20 km from the ridge axis and are given in 10^6 grams per year and centimeter of ridge axis. Increase in permeability causes stronger convection and thus higher mass fluxes. The calculated mass fluxes range between 1 and $5 \cdot 10^6$

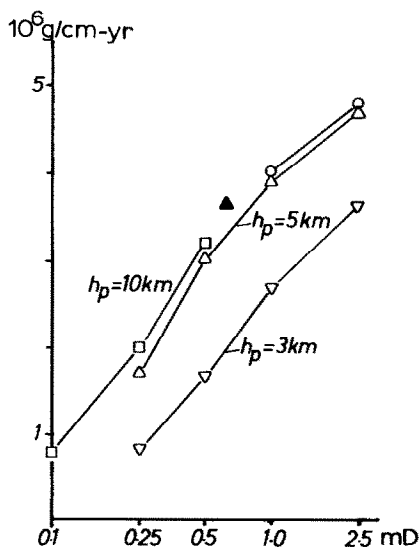


Fig. 11. Steady state fluid mass fluxes through the surface of domains of various permeabilities and penetration depths, integrated over the area between 0 and 20 km distance from the ridge axis. Open circles and closed triangle as in Fig. 9.

g/cm yr. The case with fractures in the upwelling limbs of convection cells (see Fig. 8) results in a mass flux of $3.7 \cdot 10^6$ g/cm yr.

If these mass fluxes are considered as being representative for hydrothermal convection at mid-ocean ridges, the total mass of sea water convecting through all ridges can be estimated. In order to convert our results into mass fluxes through the entire ridge system, the fluxes of Fig. 11 have to be multiplied by the length of the ridge systems (50,000 km) and by a factor of 2 for symmetry. If the model of Fig. 8 is used as an example, i.e. two fractures in a domain of 0.5 mD permeability to a depth of 5 km, a mass of $3.7 \cdot 10^{16}$ g/yr convects through crust younger than 2 m.y. old. Hydrothermal convection is, however, not restricted to crust of this age, but is inferred to occur in crust as old as 70 m.y. (Anderson et al., 1977). If older crust is included into the calculations, the total hydrothermal mass flux is increased by a factor between 1.5 and 4 depending on permeability distribution and sediment coverage of older crust (Fehn and Cathles, 1978). On this basis we estimate the total mass flux associated with hydrothermal convection at mid-ocean ridges to be smaller than $2 \cdot 10^{17}$ g/yr.

This mass flux is lower by at least a factor of 2 than the mass flux suggested by Wolery and Sleep (1976). This difference could be related to the occurrence of a more rapid convection at fast spreading ridges which are not considered in our calculations. Other reasons for this difference may be that the heat loss attributed by Wolery and Sleep to hydrothermal convection seems too high in view of new heat flow investigations (Anderson et al., 1977) and that their estimate of total mass flux is based on the assumption that the entire difference between observed and predicted heat flow is lost by the exit of heated water through the ocean floor. Any vent discharging heated water is, however, surrounded by a zone of high conductive heat flow, which can be responsible for an important part of the total heat transfer associated with hydrothermal convection. If these considerations are taken into account, the result obtained here is in good agreement with Wolery and Sleep's (1976) estimate.

CONCLUSIONS

Calculations were carried out for hydrothermal convection through oceanic crust of 10 km depth and 20 km width at a mid-ocean ridge spreading at a rate of 1 cm/yr. The following results were obtained:

(1) Heat flow over areas where downwelling convection occurs is compatible with observed heat flow values at active spreading centers provided the average permeability of the crust is less than 2.5 mD.

(2) Convection in crust of uniform permeability can depress heat flow values below the values predicted by conductive models over approximately 70% of the ocean floor. The rest of the area has heat flow higher than predicted by these models. If narrow zones of high permeability exist in domains of intermediate permeability, the percentage of zones with heat flow

lower than predicted is increased to more than 90% of the area. Since this latter result is in good agreement with the observed distribution of depressed and increased heat flow values near mid-ocean ridges, we suggest a model in which downwelling convection occurs in wide areas of the sea floor where the crust has permeabilities between 0.25 and 2.5 mD while upwelling flow is concentrated in narrow zones of considerably higher permeability.

(3) If the oceanic crust is not hydrothermally altered entirely or nearly entirely within the first two million years of its existence, the reasonably good agreement between observed ridge elevations and those expected from depth-age relations suggests that fluid circulation is restricted to depths smaller than 5 km in crust less than two million years old.

(4) Temperatures in the portions of the crust where hydrothermal convection occurs are generally lower than 400°C and reach values above 500°C in areas close to the ridge axis only.

(5) If circulation to a depth of 5 km is allowed, and the average crustal permeability is 1 mD, $4 \cdot 10^6$ g of water circulate per year through each cm wide and 20 km long strip of oceanic crust perpendicular to a ridge crest spreading at 1 cm/yr. If all ridges are similar to those spreading at 1 cm/yr, $4 \cdot 10^{16}$ g of water circulate through the oceanic crust within 20 km of all ridge crests each year. Up to $2 \cdot 10^{17}$ g/yr may circulate through the oceanic crust taking into account crust older than two million years. These mass fluxes are somewhat lower than those estimated by Wolery and Sleep (1976), but, for reasons cited in the text, can be considered in good agreement with Wolery and Sleep's estimate.

ACKNOWLEDGEMENTS

We are grateful to H.D. Holland for his support of the project and for many helpful discussions. We also thank K.E. Green for making available the unpublished heat flow data from the Galapagos Spreading Center. The second author wishes to thank Kennecott Copper Corporation for its support of the project. The research was funded by the National Science Foundation, Grant OCE 76-82188.

REFERENCES

- Anderson, R.N., Langseth, M.G. and Sclater, J.G., 1977. The mechanism of heat transfer through the floor of the Indian Ocean. *J. Geophys. Res.*, 82: 3391-3409.
- Ballard, R.D. and Van Andel, T.H., 1977. Morphology and tectonics of the inner rift valley at lat 36° 50' N on the Mid-Atlantic Ridge. *Geol. Soc. Am. Bull.*, 88: 507-530.
- Bodvarsson, G. and Lowell, R.P., 1972. Ocean-floor heat flow and the circulation of interstitial waters. *J. Geophys. Res.*, 77: 4472-4475.
- Bryant, W.R., Deflache, A.P. and Trabant, P.K., 1974. Consolidation of marine clays and carbonates. In: A.L. Interbitzen (Editor), *Deep-Sea Sediments: Physical and Mechanical Properties*. Plenum, New York, N.Y., pp. 209-244.
- Carnahan, B., Luther, H.A. and Wilkes, J.O., 1969. *Applied Numerical Methods*. Wiley, New York, N.Y., pp. 604.

- Cathles, L.M., 1977. An analysis of the cooling of intrusives by ground-water convection which includes boiling. *Econ. Geol.*, 72: 804–826.
- Coleman, R.G. and Keith, T.E., 1971. A chemical study of serpentinization — Burro Mountain, California. *J. Petrol.*, 12: 311–328.
- Crane, K. and Normark, W.R., 1977. Hydrothermal activity and crestal structure of the East Pacific Rise at 21°N. *J. Geophys. Res.*, 82: 5336–5348.
- Davis, E.E. and Lister, C.R.B., 1974. Fundamentals of ridge topography. *Earth Planet. Sci. Lett.*, 21: 405–413.
- Davis, E.E. and Lister, C.R.B., 1977. Heat flow measured over the Juan de Fuca Ridge: evidence for widespread hydrothermal circulation in a highly heat transportive crust. *J. Geophys. Res.*, 82: 4845–4860.
- Fehn, U. and Cathles, L.M., 1978. Hydrothermal convection through oceanic crust between 0 and 70 m.y. old. *EOS, Trans., Am. Geophys. Union, Abstr.*, 59: 384.
- Katz, B.J., Harrison, C.G.A. and Man, E.H., 1977. Organic geochemical evidence for oscillatory heat flow on the Mid-Atlantic Ridge (abstr.). *EOS, Trans., Am. Geophys. Union*, 58: 514.
- Lister, C.R.B., 1972. On the thermal balance of a mid-ocean ridge. *Geophys. J.R. Astron. Soc.*, 26: 515–535.
- Lister, C.R.B., 1974. On the penetration of water into hot rock. *Geophys. J.R. Astron. Soc.*, 39: 465–509.
- Lister, C.R.B., 1977. Qualitative models of spreading-center processes including hydrothermal penetration. *Tectonophysics*, 37: 203–218.
- Lowell, R.P., 1975. Circulation in fractures, hot springs, and convective heat transport on mid-ocean ridge crests. *Geophys. J.R. Astron. Soc.*, 40: 351–365.
- Lowell, R.P. and Patterson, P.L., 1979. Numerical models of hydrothermal circulation at an ocean ridge axis. In: F.T. Manheim and K. Fanning (Editors), *The Dynamic Environment of the Sea Floor*.
- Lowell, R.P., Patterson, P.L. and Fulford, J.K., 1977. Numerical modeling of hydrothermal circulation at slow spreading ridges (abstr.). *Geol. Soc. Am., Abstr. Progr.*, 9: 1075–1076.
- Moore, J.G., Fleming, H.S. and Phillips, J.D., 1974. Preliminary model for the extrusion and rifting at the axis of the Mid-Atlantic Ridge, 36°48' North. *Geology*, 2: 437–450.
- Morgan, W.J., 1975. Heat flow and vertical movement of the crust. In: A.G. Fischer and S. Judson (Editors), *Petroleum and Global Tectonics*. Princeton Univ. Press, Princeton, N.J., 23–43.
- Oldenburg, D.W., 1975. A physical model for the creation of the lithosphere. *Geophys. J.R. Astron. Soc.*, 43: 425–451.
- Parsons, B. and Sclater, J.G., 1977. An analysis of the variation of ocean floor bathymetry and heat flow with age. *J. Geophys. Res.*, 82: 803–827.
- Pearson, W.C. and Lister, C.R.B., 1973. Permeability measurements on a deep sea core. *J. Geophys. Res.*, 78: 7786–7787.
- Ribando, R.J., Torrance, K.E. and Turcotte, D.L., 1976. Numerical models for hydrothermal circulation in the oceanic crust. *J. Geophys. Res.*, 81: 3007–3012.
- Von Herzen, R., Green, K.E. and Williams, D., 1977. Hydrothermal circulation at the Galapagos Spreading Center (abstr.). *Geol. Soc. Am., Abstr. Progr.*, 9: 1212–1213.
- Williams, D.L. and Von Herzen, R.P., 1974. Heat loss from the Earth: new estimate. *Geology*, 2: 327–328.
- Williams, D.L., Von Herzen, R.P., Sclater, J.G. and Anderson, R.N., 1974. The Galapagos spreading center: lithospheric cooling and hydrothermal circulation. *Geophys. J.R. Astron. Soc.*, 38: 587–608.
- Williams, D.L., Lie, T-C., Von Herzen, R.P., Green, K.E. and Hobart, M.A., 1977. A geothermal study of the Mid-Atlantic Ridge near 37°N. *Geol. Soc. Am. Bull.*, 88: 531–540.
- Wolery, T.J. and Sleep, N.H., 1976. Hydrothermal circulation and geochemical flux at mid-ocean ridges. *J. Geol.*, 84: 249–275.